Desalination and Water Treatment
www.deswater.com

doi: 10.5004/dwt.2023.29775

303 (2023) 24–33
August

Role of the temperature gradient in the power generation performance of reverse electrodialysis in conical nanochannels

Gensheng Wu[a,*], Jiahao Shen[a], Weiyu Chen[a], Zhishan Yuan[b], Yu Bo[c,*]

[a]*College of Mechanical and Electronic Engineering, Nanjing Forestry University, Nanjing 210037, China, emails: genshengwu@njfu.edu.cn (G. Wu), 1791957295@qq.com (J. Shen), wychen@njfu.edu.cn (W. Chen)*
[b]*School of Electromechanical Engineering, Guangdong University of Technology, Guangzhou 510006, China, email: zhishanyuan@gdut.edu.cn (Z. Yuan)*
[c]*College of Science, Nanjing Forestry University, Nanjing 210037, China, email: Boyu@njfu.edu.cn (B. Yu)*

Received 13 February 2023; Accepted 14 July 2023

ABSTRACT

Reverse electrodialysis in nanochannels has become an innovative method to obtain clean energy. To enhance the power generation efficacy of the nanochannel, the finite element method was employed to model the impact of the temperature gradient on the power generation efficiency of the conical channel. The investigation primarily focused on the nanochannel structure, as well as the direction and magnitude of the solution temperature gradient. The results show that the overall power generation performance is superior for ions diffusing from the large pore end to the small pore end in the presence of a negatively charged wall surface. The nanochannel system with a negative temperature gradient shows better power generation performance than that with a positive temperature gradient under the same nanochannel parameters and solution conditions.

Keywords: Reverse electrodialysis; Temperature gradients; Conical nanochannels

1. Introduction

To date, various problems have arisen, such as energy crises and climate warming, which necessitate corresponding sustainable, environmentally friendly methods to generate energy, which mainly include solar energy, geothermal energy, wind energy, bioenergy, and tidal energy [1–4]. The ocean contains large amounts of energy; for example, the concentration difference between saline water and fresh water at the interface of rivers and seawater can be harvested and converted into electricity; this energy is called blue energy [5–7]. It is estimated that approximately 0.8 kWh·m^{-3} of energy can be extracted from the mixing of river water and seawater [8,9], and the world's available blue energy can exceed 1.4 TW [10]. To realize this, a reverse electrodialysis (RED) power generation system has been proposed by utilizing a porous membrane to separate two saline solutions of different concentrations. Due to the development of nanoprocessing technology [11], nanochannels have been widely applied in the development of RED systems [12–15]. Due to the concentration difference, saline ions are driven to migrate from the high concentration end to the low concentration end; then, by connecting the two ends of the membrane, a net current is generated due to the difference in the transport of cations and anions, and Gibbs free energy can be converted into electricity [16–18]. Until now, generating net current has mainly been accomplished because the charged surface of the nanochannel attracts counterions and repels co-ions, which forms an electric double layer (EDL) [19,20]. When the ions pass through the nanochannel, the flux of anions and cations in the EDL region is not equal, which reflects the selectivity of the ions, and a net current is generated. It is obvious that EDL has a great influence on the net current. A thicker EDL can lead to

* Corresponding authors.

stronger ion selectivity and a larger net current. In addition to the ion selectivity, the net current is also affected by ion flux. In previous studies, the effects of ion selectivity and ion flux were often competitive [21]. To balance the relationship between ion selectivity and permeability, researchers have proposed an asymmetric channel [22–24]; the diameter of one end of the asymmetric nanochannel is several nanometers wide, and the other end's diameter is hundreds of nanometers wide. The asymmetric structure can help to reduce the internal resistance of the nanochannel to ensure high ion selectivity so that the power generation system has high ion selectivity and ion flux at the same time. Conical channels are typical asymmetric nanochannels, and the power generation performance of conical nanochannels has been extensively studied in recent years. Yeh et al. [22] investigated RED power generation in negatively charged conical nanopores by numerical simulations and found that a high EDL overlapping degree was achieved with a low concentration in the small pore end and a high concentration in the large pore end to obtain superior power generation performance of RED. Furthermore, they also investigated the influence of different ion species, including KCl, NaCl and LiCl salt solutions. Due to the difference between the diffusion coefficients of anions and cations, the power generation performance varies for different solutions. Better power generation performance is shown at low concentrations with higher diffusion coefficients of cations, and the opposite behavior is shown at high concentrations.

In addition to the type of ion species, the diffusion coefficient can also be affected by the solution temperature, which can further influence the power generation performance of conical nanochannels. Tseng et al. [25] analyzed the influence of temperature and found that only the ion flux is affected by equal temperatures on both sides of the nanochannel, which has little effect on ion selectivity. However, compared with this equal temperature system, unequal temperature can further amplify the power generated by creating a temperature gradient, which, to the best of our knowledge, has not been studied before. In this work, the directions of the temperature gradient and concentration gradient are comprehensively investigated to provide a clue for designing the RED power generation system.

2. Theory

Fig. 1 shows the dimensional symmetric model based on the principle of the RED power generation system. Two solution reservoirs are connected with a conical nanochannel, where C_L is the concentration at the low concentration end and C_H is the concentration at the high concentration end. T_H is the temperature at the high concentration end, and T_L is the temperature at the low concentration end. h, R_H, and R_L are the nanochannel length, radius at the high concentration end and radius at the low concentration end, respectively. R_r and L_z are the radius and length of the solution reservoirs, respectively. Then, a series of equations consisting of Poisson–Nernst–Planck and Navier–Stokes describing the relationship among ion concentration, electric field, and fluid flow rate were used for the analysis [26–28]. The relationship between potential and ion concentration is described by:

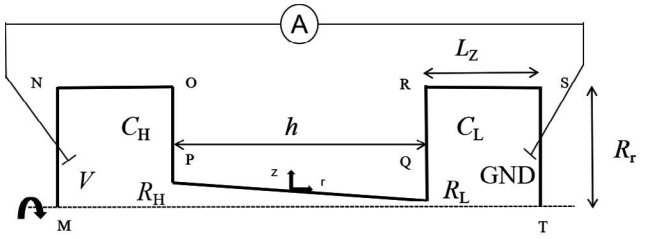

Fig. 1. Schematic diagram of a conical nanochannel with a salinity gradient for power generation.

$$-\varepsilon_0\varepsilon_\gamma\nabla^2\varphi=\rho_e=\sum_{i=1}^{2}Fz_ic_i \tag{1}$$

where ρ_e is the charge density, φ is the electrical potential, F is the Faraday constant, z_i is the number of charges carried by the ion, c_i is the ion concentration, ε_r is the dielectric constant of the solution, and ε_0 is the vacuum dielectric constant.

Eq. (2) is the flux equation for each ion in the steady-state system, which describes the transport properties of the charged nanopore and includes the calculation of the ion convective flux, electromigration flux, diffusion flux and thermal diffusion flux, where convective flux originates from ionic convection effects caused by solution flow. The diffusion flux comes from the effect of the concentration gradient in space, and the diffusion current is generated as the anion and cation diffusion coefficients or concentration gradients are different. The electromigration flux is the movement of ions caused by the mutual coupling of the electric field of the EDL and the applied electric field, generating the electromigration current. Compared with the diffusion current and electrodiffusion current, the current contribution of the thermal flux effect can be neglected [29].

$$\nabla\cdot J_i=\nabla\cdot\left[uc_i-D_i\nabla c_i-\frac{z_iF}{RT}D_ic_i\nabla\varphi-\frac{2D_i\alpha_ic_i}{T}\nabla T\right]=0 \tag{2}$$

where u is the flow rate of the fluid, D_i is the diffusion coefficient of the ion, α_i is the reduced Soret coefficient and R is the gas constant in the environment.

$$-\nabla p+\mu\nabla^2u-\rho_e\nabla\varphi-\frac{1}{2}\varepsilon_0\left|-\nabla\varphi\right|^2\nabla\varepsilon_\gamma=0 \tag{3}$$

Eq. (3) is the equation of motion describing the conservation of fluid momentum, where μ and ρ are the fluid viscosity and pressure, respectively. The fluid flows steadily in the direction of the nanochannel, satisfying Eq. (4):

$$\nabla\cdot u=0 \tag{4}$$

Eq. (5) is the heat transfer equation:

$$\rho C_pu\cdot\nabla T=\nabla\cdot\left(k\nabla T\right) \tag{5}$$

where ρ, C_p and k represent the density, specific heat capacity and thermal conductivity of the solution, respectively.

The numerical simulation was performed by using COMSOL Multiphysics software, and the boundary conditions were set according to Table 1 with the following parameters: ε_r = 80 F·m^{-1}, F = 96,485 C·mol^{-1}, R = 8.314 J·K^{-1}·mol^{-1}. KCl solution is applied as the power generation source solution, and its parameters can be referenced in Eqs. (S1)~(S5). The wall surface charge density ρ_e was set to –5 mC·m^{-2}. C_L was always set to 1 mmol·L^{-1}. The ratio of the high concentration end to the low concentration end is expressed as $C_H|C_L$. Model validation was conducted by checking the grid independence, as shown in Fig. S1. To verify the validity of the model in this paper, the net current and cation transport factor calculated by the model of Cao et al. [30] were compared after the mesh-independent model, as shown in Fig. S2. The output parameters include the net current, open circuit voltage, maximum power and maximum power efficiency, which can be found in Eqs. (S6)–(S18).

Fig. 2a and b show the different ion diffusion behaviors of the RED power generation system for $R_H > R_L$ and $R_H < R_L$, respectively. The directions of ion diffusion are consistent, and $R_H \neq R_L$. According to EDL theory, ion selectivity is mainly determined by EDL overlap, which has a strong effect on ion transport near the low concentration end of the nanochannel. For $R_H > R_L$, high selectivity is shown due to the EDL overlapping in the small pore end at low concentrations compared with that for $R_H < R_L$, which can be observed by comparing Fig. S4a and c. The direction of the temperature gradient is the same as that of the concentration gradient ($T_H > T_L$), defined as a positive temperature gradient (PTG). The ion diffusion coefficient decreases along the diffusion direction for PTG and thus suppresses ion diffusion. Ions are then aggregated inside the nanochannel, and a high ion concentration leads to a thinner EDL. Conversely, a negative temperature gradient (NTG) indicates that $T_H < T_L$ can promote ion diffusion in low-concentration nanochannels in which the overlapping degree is higher. Therefore, the ion selectivity is stronger in NTG, which can be found by comparing Fig. S4a and b or Fig. S4c and d. To avoid the size effect on ion transport in the nanochannel, the R_r and L_z of the reservoir are set to 500 nm.

3. Results and discussion

3.1. Influence of the temperature gradient on the net current generated by the RED power generation system of conical nanochannels

Fig. 3 shows the net current generated by the RED power generation system in conical nanochannels with different concentration gradients and temperature gradients. In

Table 1
Boundary conditions of the model

Surface	Electric potential	Ion transport	Flow field	Heat transfer
MN	Constant voltage	Low concentration (C_H)	Pressure = 0	T_H
NO, RS	Zero charge	Symmetry	Symmetry	Symmetry
OP, QR, PQ	Surface charge density	No flux	No slip	Thermal insulation
ST	Ground	High concentration (C_L)	Pressure = 0	T_L
TM	Axisymmetric	Axisymmetric	Axisymmetric	Axisymmetric

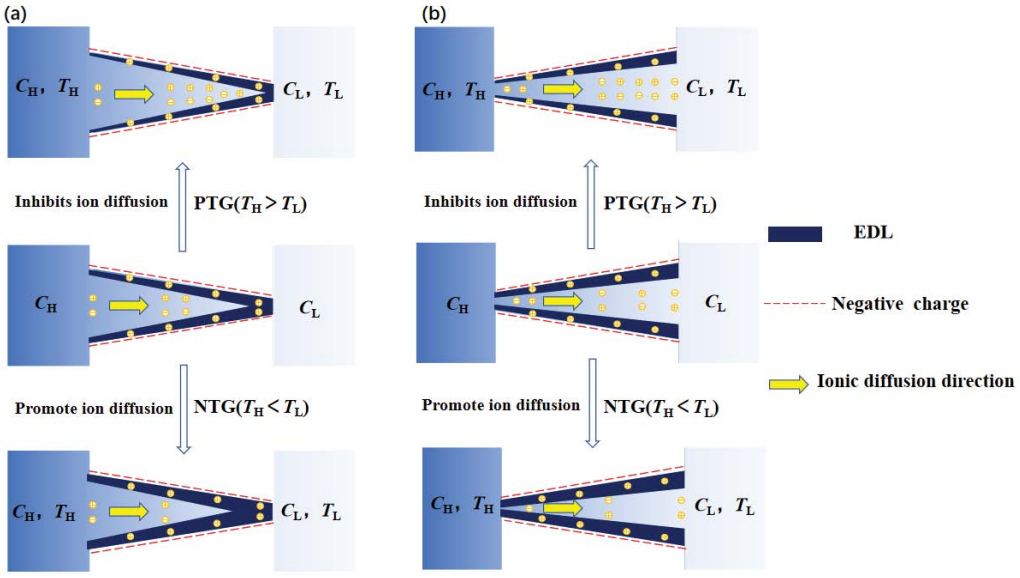

Fig. 2. Schematic diagram of RED power generation with conical nanochannels with different temperature gradients. (a) $R_H > R_L$ and (b) $R_H < R_L$.

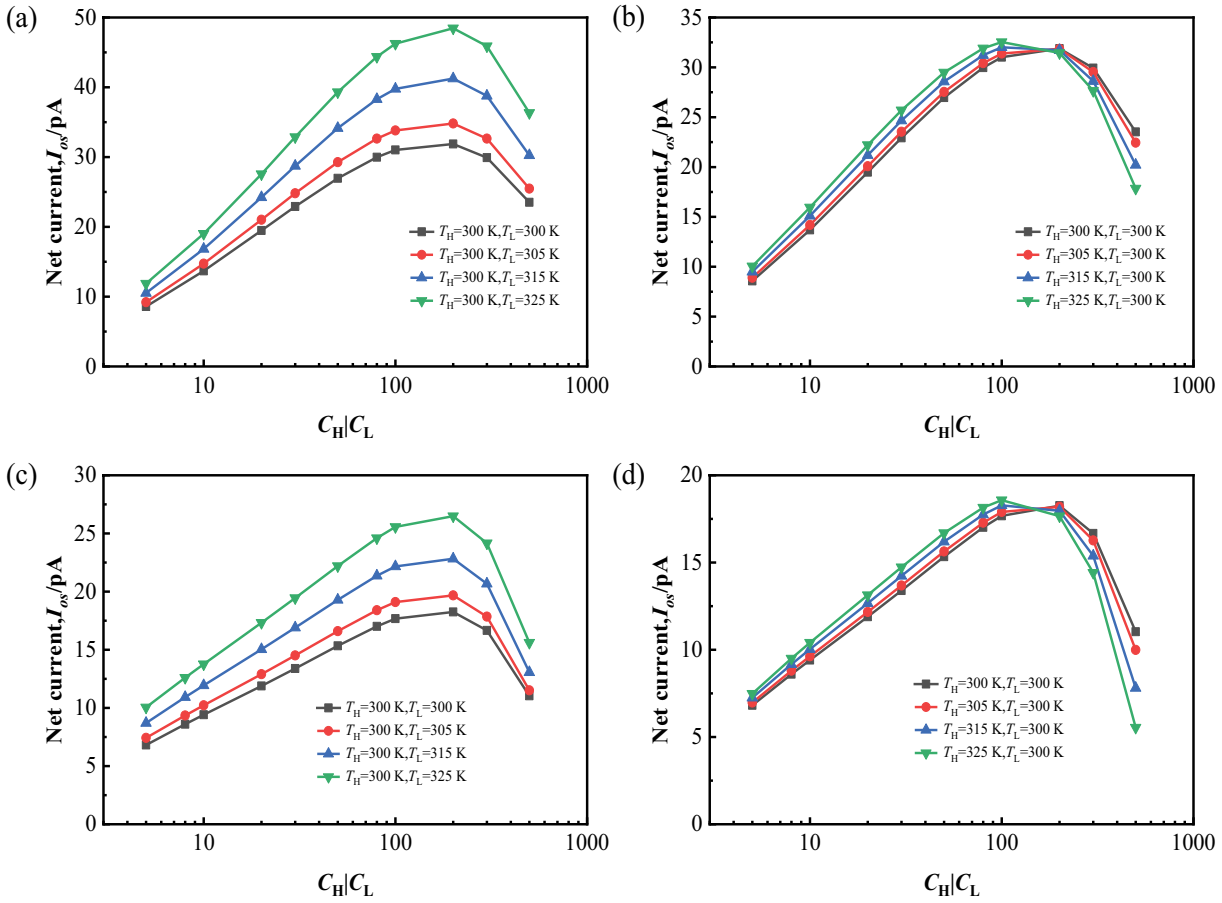

Fig. 3. Variation in the net current generated by the conical nanochannel RED power generation with the concentration gradient at different temperature gradients ($C_H|C_L$ = 5~500). (a) NTG, R_H = 100 nm, R_L = 10 nm, h = 500 nm, (b) PTG, R_H = 100 nm, R_L = 10 nm, h = 500 nm, (c) NTG, R_H = 10 nm, R_L = 100 nm, h = 500 nm, and (d) PTG, R_H = 10 nm, R_L = 100 nm, h = 500 nm.

general, the net current first increases and then decreases as the concentration ratio increases. The ion flux increases, but the ion selectivity gradually decreases as the concentration ratio increases. For NTG, the peak value (49.68 pA) occurs at approximately $C_H|C_L$ = 300, T_H = 300 K, and T_L = 325 K for $R_H > R_L$. It is also noted that the net current can be affected by the nanochannel structure and the direction of the temperature gradient. The net current is larger for $R_H > R_L$ and a NTG when the other parameters are kept the same because the net current is mainly determined by the ion selectivity of the nanochannel at a constant ion flux, and the ion selectivity of the cation is higher for $R_H > R_L$ and a NTG, as also shown in Fig. 2. Furthermore, the magnitude of the temperate gradient also has an obvious influence on power generation performance. According to Fig. S5, the diffusion coefficient of anions is increased by increasing the temperature, and the ion flux is promoted. Fig. 4a shows that ion migration can be enhanced by increasing the negative temperature gradient, and the ion concentration inside the nanochannel is lower. Thus, the ion selectivity is stronger, as shown in Fig. S4a and c. With the combined effects of ion flux and ion selectivity, the net current is enhanced by the increased negative temperature gradient, as shown in Fig. 3a and c. For the PTG, ion migration is inhibited by a positive temperature gradient, and ions will accumulate inside the nanochannel, leading to a high ion concentration. With an increased temperature gradient, the ion concentration increases, and the ion selectivity becomes weaker, as shown in Fig. 4b. Since the effect of ion flux is competitive with that of ion selectivity, the net current has no obvious change with increasing temperature gradient, as shown in Fig. 3b and d. Apparently, the net current enhancement is more dependent on the ion flux increase, and the net current increases with increasing temperate gradient. Conversely, the effect of ion selectivity is more obvious at high concentrations, in which the net current decreases as the temperate gradient increases.

3.2. Influence of the temperature gradient on the open circuit voltage generated by the RED power generation system of conical nanochannels

According to S8, the open circuit voltage depends on the cation transport factor, concentration ratio and temperature. As shown in Fig. 5, the open circuit voltage first increases and then decreases as the concentration increases, and the maximum value can reach 0.0358 V at T_H = 300 K, T_L = 325 K, $R_H > R_L$ and $C_H|C_L$ = 10. For the same concentration ratio and temperature gradient, the open circuit voltage

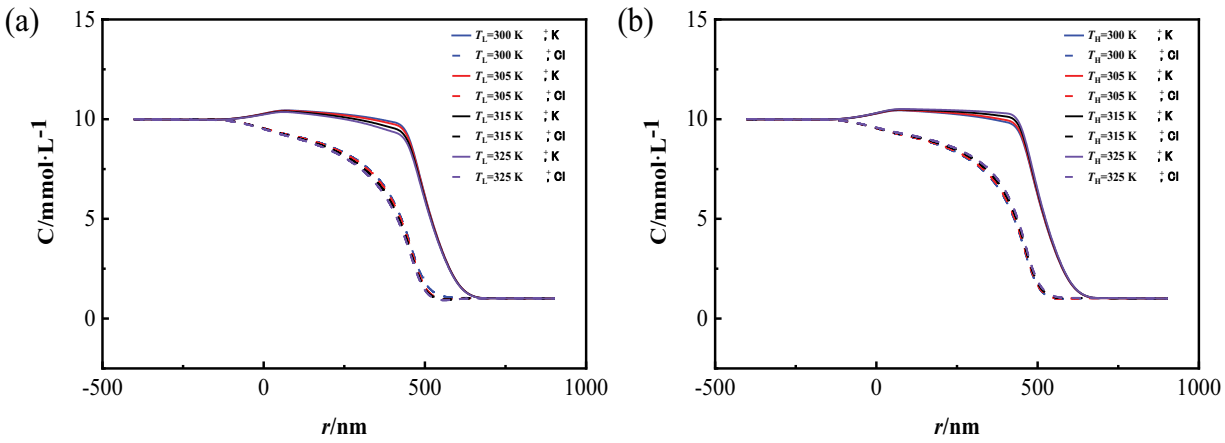

Fig. 4. Concentrations of K^+ (solid line) and Cl^- (dotted line) in the r direction at different temperature gradients for R_H = 100 nm, R_L = 10 nm, h = 500 nm, and T_H = 300 K. (a) NTG, $C_H|C_L$ = 10|1 and (b) PTG, $C_H|C_L$ = 10|1.

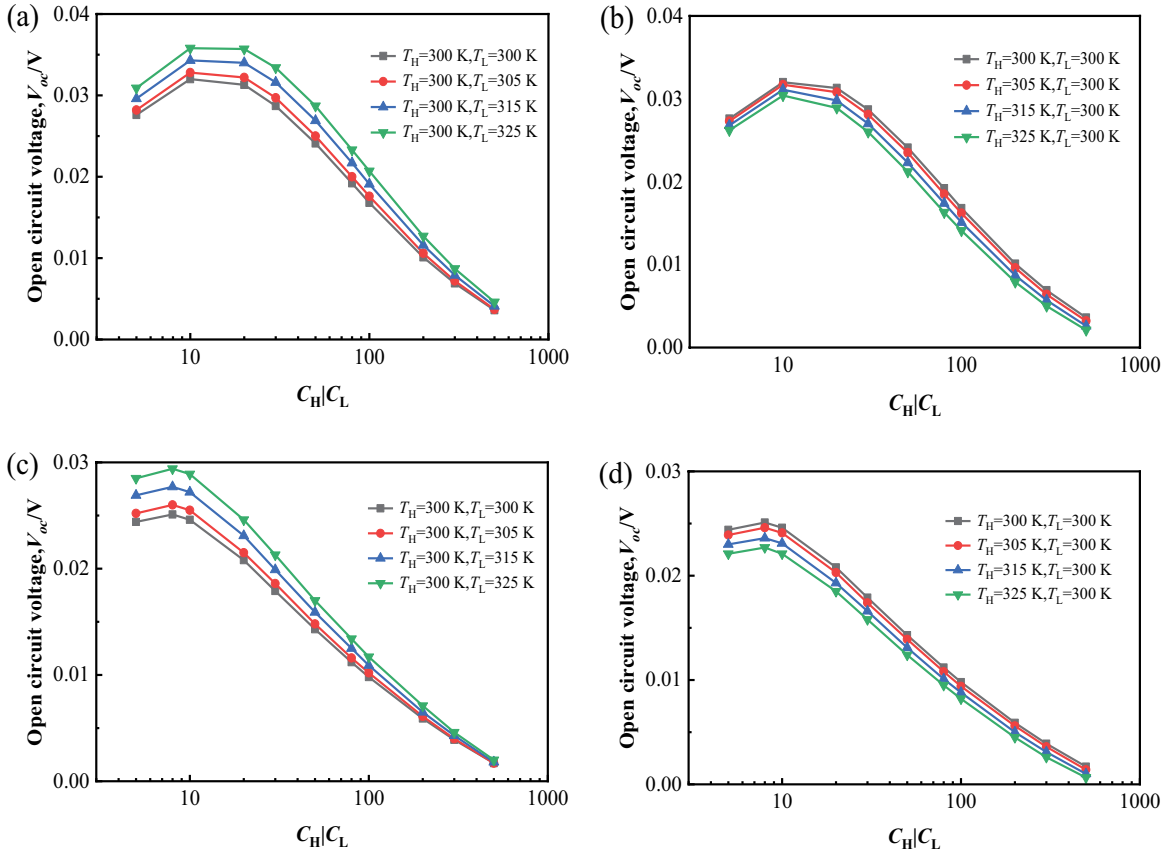

Fig. 5. Variation in the open-circuit voltage in the conical nanochannel RED power generation system with the concentration gradient at different temperature gradients. (a) NTG, R_H = 100 nm, R_L = 10 nm, h = 500 nm, (b) PTG, R_H = 100 nm, R_L = 10 nm, h = 500 nm, (c) NTG, R_H = 10 nm, R_L = 100 nm, h = 500 nm, and (d) PTG, R_H = 10 nm, R_L = 100 nm, h = 500 nm.

would be larger for NTG and $R_H > R_L$, which only depends on the cation transport factor. It is also found that the influence of the temperature gradient on the open circuit voltage is mainly due to ion selectivity in the NTG and PTG, which can be observed by comparing Figs. 5 and S4. The magnitude of the temperature has little effect on the open circuit voltage, and the variation trend of the open circuit voltage is almost the same as that of the ion selectivity. For the NTG, the open circuit voltage increases as the temperature gradient increases, as shown in Fig. 5a and c. For the PTG, the open circuit voltage decreases as the temperature gradient increases, as shown in Fig. 5b and d.

3.3. Influence of the temperature gradient on the maximum power generated by RED in conical nanochannels

Fig. 6 shows the maximum power with the change in concentration gradient at different temperature gradients in a conical nanochannel RED power generation system. According to Eq. (S9), the maximum power is directly affected by the net current and open circuit voltage, and the maximum power first increases and then decreases as the concentration gradient increases for all temperature gradients. With the same conditions, the net current and open circuit voltage reach the highest values so that the maximum power is largest for $R_H > R_L$ and NTG. The maximum power is influenced more by the temperature gradient because the net current and open circuit voltage both increase in a NTG, and the net current is relatively greatly enhanced, as shown in Fig. 6a and c. For the PTG, the net current increases slightly as the temperature gradient increases at low concentrations, while the open circuit voltage decreases; thus, the maximum power has almost no change at low concentrations. At high concentrations, the net current and open circuit voltage both decrease with increasing temperature gradient so that the maximum power is decreased. In other words, the maximum power is highest (0.28 pW) with $C_H|C_L = 50$, $T_H = 300$ K and $T_L = 325$ K for $R_H > R_L$.

3.4. Influence of the temperature gradient on the maximum power efficiency generated by RED in conical nanochannels

According to Eq. (S17), the maximum power efficiency is related to the cation selectivity and the Gibbs free energy loss. As shown in Fig. 7, the maximum power efficiency decreases to 0 as the concentration gradient increases, mainly due to the decreased cation selectivity of the nanochannels at high concentrations. Due to the effect of ion selectivity, the maximum power efficiency of $R_H > R_L$ is higher than that for $R_H < R_L$ when the other parameters are kept the same. According to Eq. (S10), the difference in chemical potential is clearly lower for the NTG than for the PTG, which leads to a smaller Gibbs free energy loss. Furthermore, the ion selectivity for the NTG is higher than that for the PTG, so the maximum power efficiency is higher according to Eq. (S17). Considering the magnitude of the temperature gradient, as the NTG increases, the Gibbs free energy of the system will further decrease, and the cation selectivity is also enhanced; thus, the maximum power efficiency is promoted, as shown in Fig. 7a and c. For the PTG, the Gibbs free energy loss increases and the cation selectivity decreases as the PTG increases, which can lead to a decrease in the maximum power efficiency.

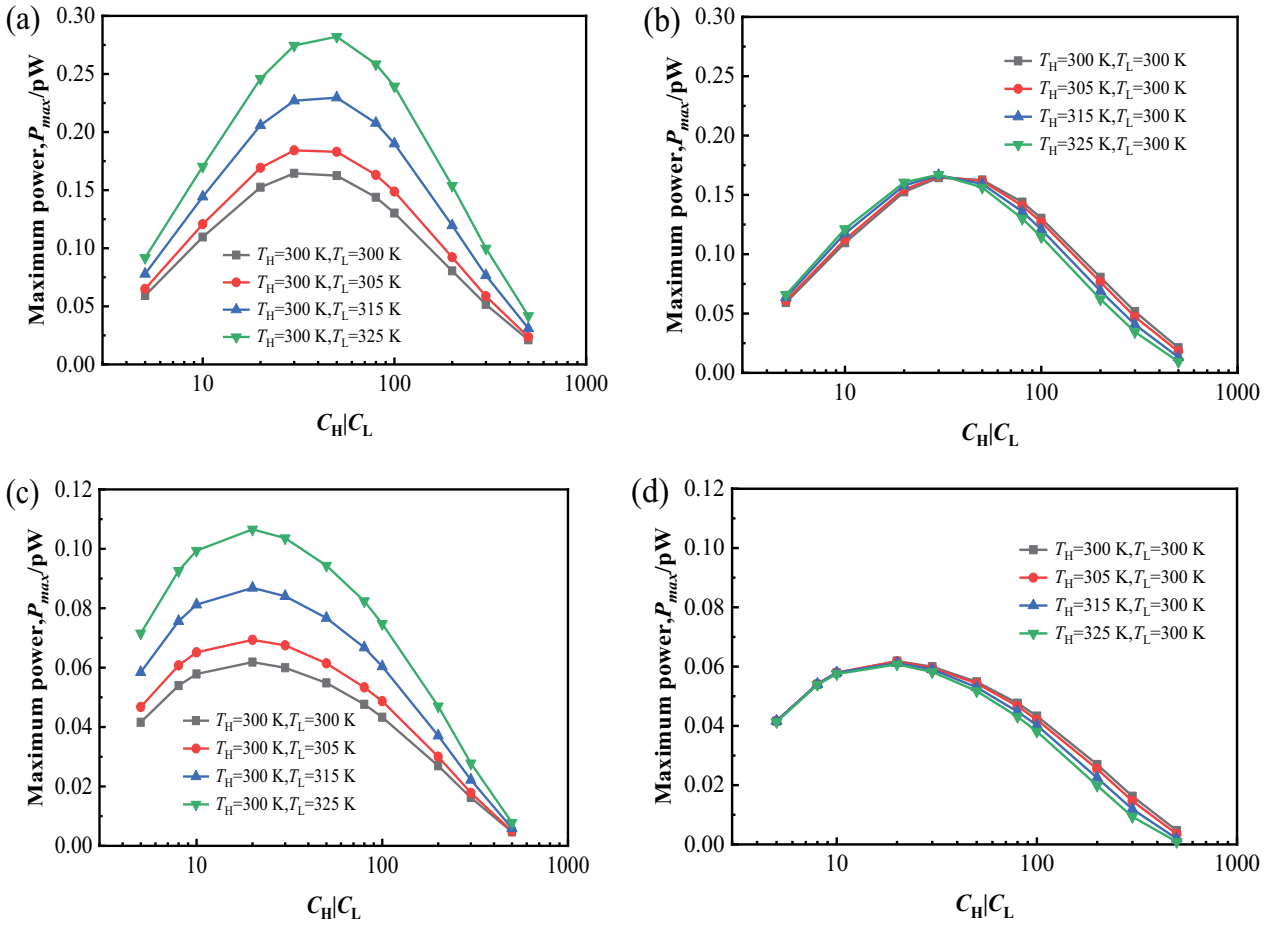

Fig. 6. Variation in the maximum power of the conical nanochannel RED power generation system with different concentration and temperature gradients. (a) NTG, R_H = 100 nm, R_L = 10 nm, h = 500 nm, (b) PTG, R_H = 100 nm, R_L = 10 nm, h = 500 nm, (c) NTG, R_H = 10 nm, R_L = 100 nm, h = 500 nm, and (d) PTG, R_H = 10 nm, R_L = 100 nm, h = 500 nm.

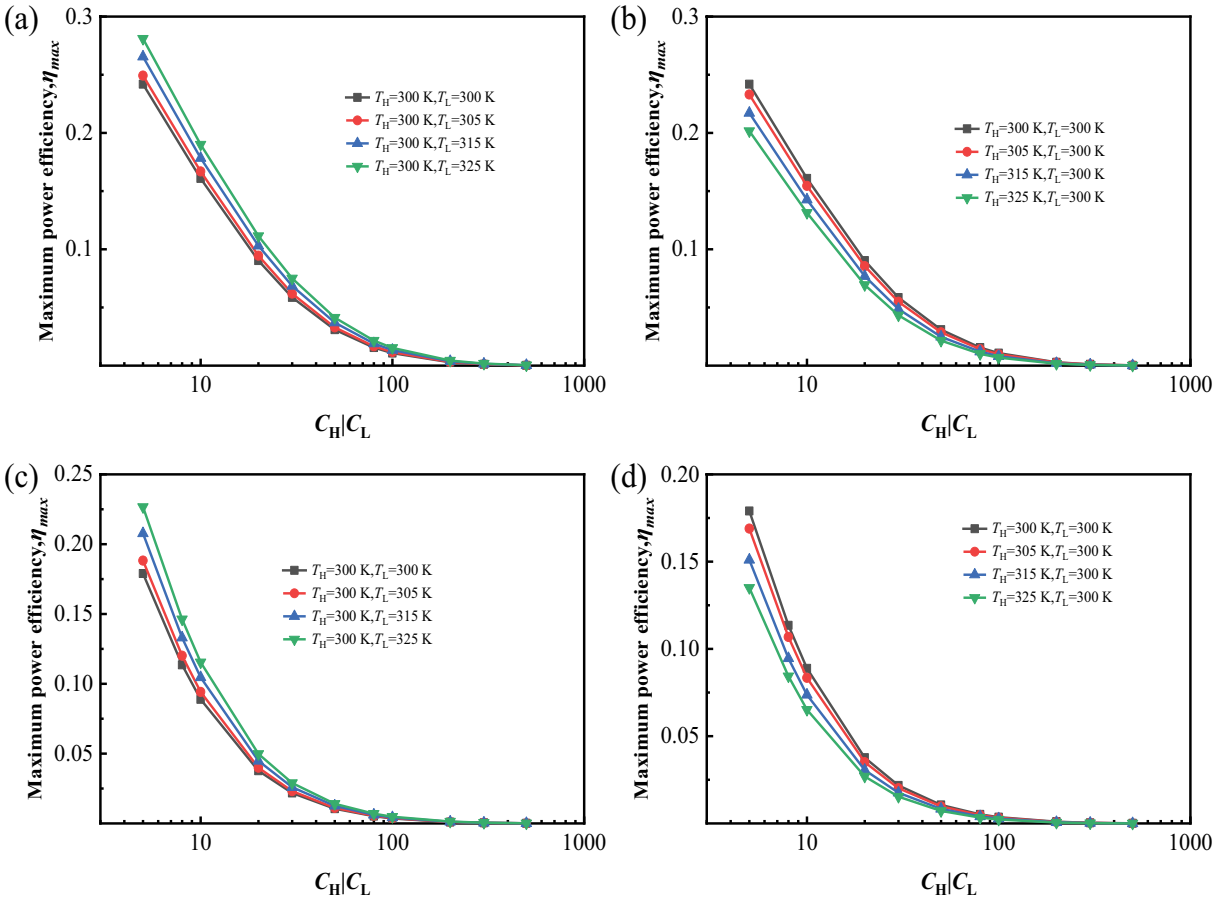

Fig. 7. Variation in the maximum power efficiency generated by the conical nanochannel RED power generation with the concentration gradient at different temperature gradients. (a) NTG, R_H = 100 nm, R_L = 10 nm, h = 500 nm, (b) PTG, R_H = 100 nm, R_L = 10 nm, h = 500 nm, (c) NTG, R_H = 10 nm, R_L = 100 nm, h = 500 nm, and (d) PTG, R_H = 10 nm, R_L = 100 nm, h = 500 nm.

4. Conclusions

In this work, the effects of the temperature gradient on the RED performance in conical nanochannels were evaluated by using the finite element method, such as the net current, open circuit voltage, maximum power and maximum power efficiency. First, the maximum power of the RED power generation system for the NTG is larger than that for the PTG due to the direction of the temperature gradient. Second, an increased temperature gradient can increase the ion flux and promote the ion selectivity of the nanochannel, which can improve the maximum power for a NTG. However, the increased temperature gradient increases the ion flux but decreases the ion selectivity, so the maximum power cannot be promoted further for a PTG. The results indicated that the direction of the temperature gradient should be combined with the direction of the concentration gradient and the open pore direction of the conical nanochannel. This work can provide some guidelines for the design of nanochannel-based RED systems.

Acknowledgments

This work was supported by the National Natural Science Foundation of China (51905276) and Natural Science Foundation of Jiangsu Province (BK20200787).

References

[1] S. Chu, Y. Cui, N. Liu, The path towards sustainable energy, Nat. Mater., 16 (2017) 16–22.
[2] S. Chu, A. Majumdar, Opportunities and challenges for a sustainable energy future, Nature, 488 (2012) 294–303.
[3] J. Fang, J. Zhu, Y. Shi, The responses of ecosystems to global warming, CSB, 63 (2018) 136–140.
[4] P.A. Ostergaard, N. Duic, Y. Noorollahi, H. Mikulcic, S. Kalogirou, Sustainable development using renewable energy technology, Renewable Energy, 146 (2020) 2430–2437.
[5] M. Graf, M. Lihter, D. Unuchek, A. Sarathy, J.-P. Leburton, A. Kis, A. Radenovic, Light-enhanced blue energy generation using MoS_2 nanopores, Joule, 3 (2019) 1549–1564.
[6] G. Liu, T. Chen, J. Xu, K. Wang, Blue energy harvesting on nanostructured carbon materials, J. Mater. Chem. A, 6 (2018) 18357–18377.
[7] G. Nikolaidis, A. Karaolia, A. Matsikaris, A. Nikolaidis, M. Nicolaides, G.C. Georgiou, Blue energy potential analysis in the Mediterranean, Front. Energy Res., 7 (2019), doi: 10.3389/fenrg.2019.00062.
[8] A. Siria, M.-L. Bocquet, L. Bocquet, New avenues for the large-scale harvesting of blue energy, Nat. Rev. Chem., 1 (2017) 0091, doi: 10.1038/s41570-017-0091.
[9] N.Y. Yip, M. Elimelech, Thermodynamic and energy efficiency analysis of power generation from natural salinity gradients by pressure retarded osmosis, Environ. Sci. Technol., 46 (2012) 5230–5239.
[10] O.A. Alvarez-Silva, A.F. Osorio, C. Winter, Practical global salinity gradient energy potential, Renewable Sustainable Energy Rev., 60 (2016) 1387–1395.

[11] Z. Li, Q. Han, Y. Qiu, D. Wang, Modulation of water transport in carbon nanotubes by local charges, Carbon, 202 (2023) 83–92.
[12] S. Jiang, T. Shi, Z. Tang, S. Xi, Cost-effective fabrication of inner-porous micro/nano carbon structures, J. Nanosci. Nanotechnol., 18 (2018) 2089–2095.
[13] S.Q. Wang, Z.L. Zhang, W.Y. Huo, X.H. Zhang, F. Fang, Z.H. Xie, J.Q. Jiang, Single-crystal-like black Zr-TiO_2 nanotube array film: an efficient photocatalyst for fast reduction of Cr(VI), Chem. Eng. J., 403 (2021) 126331, doi: 10.1016/j.cej.2020.126331.
[14] S.Q. Wang, Z.L. Zhang, W.Y. Huo, X.H. Zhang, F. Fang, Z.H. Xie, J.Q. Jiang, Preferentially oriented Ag-TiO_2 nanotube array film: an efficient visible-light-driven photocatalyst, J. Hazard. Mater., 399 (2020) 123016, doi: 10.1016/j.jhazmat.2020.123016.
[15] T.Z. Wang, L. Huang, J.X. Pei, X.J. Hu, H.F. Jiang, Efficient water desalination using Bernoulli effect, Desal. Water Treat., 272 (2022) 37–49.
[16] B.E. Logan, M. Elimelech, Membrane-based processes for sustainable power generation using water, Nature, 488 (2012) 313–319.
[17] G.Z. Ramon, B.J. Feinberg, E.M.V. Hoek, Membrane-based production of salinity-gradient power, Energy Environ. Sci., 4 (2011) 4423–4434.
[18] S.E. Skilhagen, Osmotic power - a new, renewable energy source, Desal. Water Treat., 15 (2010) 271–278.
[19] A. Siria, P. Poncharal, A.L. Biance, R. Fulcrand, X. Blase, S.T. Purcell, L. Bocquet, Giant osmotic energy conversion measured in a single transmembrane boron nitride nanotube, Nature, 494 (2013) 455–458.
[20] J. Gao, W. Guo, D. Feng, H. Wang, D. Zhao, L. Jiang, High-performance ionic diode membrane for salinity gradient power generation, J. Am. Chem. Soc., 136 (2014) 12265–12272.
[21] L.X. Cao, F.L. Xiao, Y.P. Feng, W.W. Zhu, W.X. Geng, J.L. Yang, X.P. Chang, N. Li, W. Guo, L. Jiang, Anomalous channel-length dependence in nanofluidic osmotic energy conversion, Adv. Funct. Mater., 27 (2017) 1604302, doi: 10.1002/adfm.201604302.
[22] H.-C. Yeh, C.-C. Chang, R.-J. Yang, Reverse electrodialysis in conical-shaped nanopores: salinity gradient-driven power generation, RSC Adv., 4 (2014) 2705–2714.
[23] G. Laucirica, A.G. Albesa, M. Etoimil-Molares, Shape matters: enhanced osmotic energy harvesting in bullet-shaped nanochannels, Nano Energy, 71 (2020) 104612, doi: 10.1016/j.nanoen.2020.104612.
[24] J. Phsu, T. Csu, P.H Peng, Unraveling the anomalous surface-charge-dependent osmotic power using a single funnel-shaped nanochannel, ACS Nano, 13 (2019) 13374–13381.
[25] S. Tseng, Y.M. Li, C.Y. Lin, Salinity gradient power: influences of temperature and nanopore size, Nanoscale, 8 (2016) 2350–2357.
[26] S.Y. Noskov, W. Im, B. Roux, Ion permeation through the alpha-hemolysin channel: theoretical studies based on Brownian dynamics and Poisson–Nernst–Plank electrodiffusion theory, Biophys. J., 87 (2004) 2299–2309.
[27] C.-Y. Lin, C. Combs, Y.-S. Su, L.-H. Yeh, Z.S. Siwy, Rectification of concentration polarization in mesopores leads to high conductance ionic diodes and high-performance osmotic power, J. Am. Chem. Soc., 141 (2019) 3691–3698.
[28] F. Xiao, D. Ji, H. Li, J. Tang, Y. Feng, L. Ding, L. Cao, N. Li, L. Jiang, W. Guo, Simulation of osmotic energy conversion in nanoporous materials: a concise single-pore model, Mater. Chem. Front., 5 (2018) 1677–1682.
[29] R. Long, Z. Kuang, Z. Liu, W. Liu, Temperature regulated reverse electrodialysis in charged nanopores, J. Membr. Sci., 561 (2018) 1–9.
[30] L. Cao, Q. Wen, Y. Feng, D. Ji, H. Li, N. Li, L. Jiang, W. Guo, On the origin of ion selectivity in ultrathin nanopores: insights for membrane-scale osmotic energy conversion, Adv. Funct. Mater., 28 (2018) 1804189, doi: 10.1002/adfm.201804189.

Supporting information

S1. Model validation

S1.1. Grid setting

The model uses a triangular grid to divide the area. The relationship between the net current and the number of grid cells when using KCl solution for salt difference power generation is shown in Fig. S1. In this paper, the number of units of the model is set to 6,000.

2. Properties of KCl solutions

The KCl solution is chosen for the simulation. Since the temperature is not constant, some parameters of the solution are redefined [1].

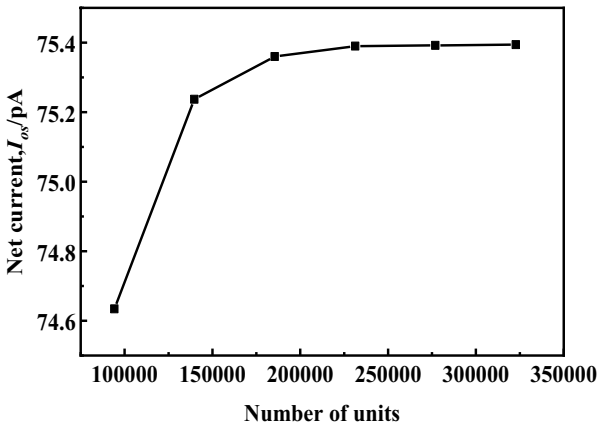

Fig. S1. Relationship between the net current and the number of grid cells for ρ_e = –10 mC·m^{-2}, L = 500 nm, R_H = 100 nm, R_L = 5 nm, h = 500 nm, $T_H|T_L$ = 300|370, $C_H|C_L$ = 200|1.

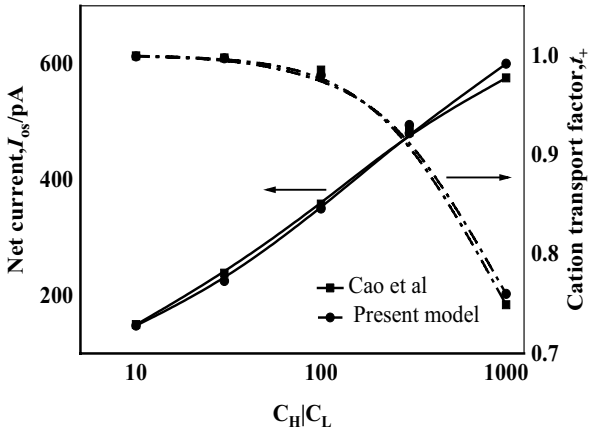

Fig. S2. Variation of net current and cation transport factor with concentration ratio for concentration gradient power generation using KCl solution for ρ_e = –60 mC·m^{-2}, h = 2 nm, R_p = 2 nm.

2.1. Relative dielectric constant

$$\varepsilon_r = \exp\left[4.4716 - 4.60128\times10^{-3}\left(\Delta T\right) + 2.6952\times10^{-7}\left(\Delta T\right)^2\right] \quad \text{(S1)}$$

where $\Delta T = T - 273.15$ and $0 \le \Delta T \le 100$.

2.2. Ion diffusion coefficient

$$D_i = \frac{RT}{F^2}\left[\frac{1/|z_i|}{1/\lambda_i^0}\right] \quad \text{(S2)}$$

$$\lambda^0_{K(dt)} = 40.5017 + 1.2194\left(dT\right) + 4.1859\times10^{-3}\left(dT\right)^2 \quad \text{(S3)}$$

$$\lambda^0_{Cl(dt)} = 76.35 + 1.54037\left(\Delta T\right) + 4.65\times10^{-3}\left(\Delta T\right)^2 - 1.285\times10^{-5}\left(\Delta T\right)^3 \quad \text{(S4)}$$

where $\Delta T = T - 273.15$, $dT = T - 298.15$.

2.3. Viscosity of the solution

$$\mu_T = 2.414\times10^{-5}\times10^{247.8/(T-140)} \quad \text{(S5)}$$

3. Output performance parameter

As shown in Fig. 2, the net current (I_{os}) is generated by the reverse electrodialysis (RED) system with no applied voltage V. Its magnitude can be calculated by:

$$I_{os} = \int_S F\left(\sum_{i=1}^{2} z_i J_i\right)\cdot nds \quad \text{(S6)}$$

where S is the cross-sectional area of the nanochannel and n is the unit normal vector. The cation transport factor (t_+) is the ratio of the current contributed by the cation to the total current which indicates the cation selectivity.

$$t_+ = \frac{I_+}{I_+ + I_-} \quad \text{(S7)}$$

where I_+ and I_- are the currents contributed by cations and anions, respectively. When $t_+ > 0.5$, the direction of the net current is positive and the channel reflects cation selectivity. The larger the t_+, the stronger the cation selectivity. As shown in Fig. S3, the ion selectivity can lead to an open circuit voltage (V_{oc}) on both sides of the nanochannel, which is equal to the applied voltage which leads to zero current of RED system [S1]. Open circuit voltage can be described by Eq. (13).

$$V_{oc} = \left|2t_+ - 1\right|\frac{RT}{zF}\ln\left(\frac{\gamma_H C_H}{\gamma_L C_L}\right) \quad \text{(S8)}$$

According to the Eq. (13), the open circuit voltage is mainly related to the cation transport factor, average temperature and concentration gradient.

The maximum power is related to the net current and the open circuit voltage, which is expressed by [S2, S3]:

$$P_{max} = \left|0.25\times I_{os}\times V_{oc}\right| \quad \text{(S9)}$$

According to the theory of thermodynamics, the Gibbs free energy decreases when ions diffuse from the high concentration end with temperature T_H and concentration C_H to the low concentration end with temperature T_L and concentration C_L is [S2]:

$$\Delta G = \Delta G_H + \Delta G_L = \left(\mu_{+,H} - \mu_{+,L}\right)n_{+,H} + \left(\mu_{-,H} - \mu_{-,L}\right)n_{-,H} \quad \text{(S10)}$$

$$\mu_{i,j} = \mu_{i,0} + RT_j\ln\beta_j \quad \text{(S11)}$$

$$n_{i,H} = -\frac{|I_i|}{F} \quad \text{(S12)}$$

where + and – represent cation (K^+) and anion (Cl^-), respectively, $\mu_{i,o}$, $n_{i,H}$ are ion chemical potential and ion flux, respectively. Gibbs free energy loss can be expressed as:

$$\Delta G = \sum_i\left(RT_H\ln\beta_{i,H} - RT_L\ln\beta_{i,L}\right)\frac{I_i}{F} \quad \text{(S13)}$$

The maximum power produced by the system is:

$$P_{max} = \left(|I_+| - |I_-|\right)V = \left(|I_+| - |I_-|\right)\frac{V_{oc}}{2} \quad \text{(S14)}$$

Then the maximum power efficiency is:

$$\eta_{max} = \frac{P_{max}}{\Delta G} = \frac{\left(|I_+| - |I_-|\right)\frac{V_{oc}}{2}}{\sum_i\left(RT_H\ln\beta_{i,H} - RT_L\ln\beta_{i,L}\right)\frac{I_i}{F}} = \frac{\left(|I_+| - |I_-|\right)\frac{V_{oc}}{2}}{\frac{R}{L}\ln\frac{\beta^{T_H}_{+,H}}{\beta^{T_L}_{+,L}}|I_+| + \frac{R}{F}\ln\frac{\beta^{T_H}_{-,H}}{\beta^{T_L}_{-,L}}|I_-|} \quad \text{(S15)}$$

where

$$\frac{\beta^{T_H}_{+,H}}{\beta^{T_L}_{+,L}} = \frac{\beta^{T_H}_{-,H}}{\beta^{T_L}_{-,L}} = \frac{\beta^{T_H}_{H}}{\beta^{T_L}_{L}} \quad \text{(S16)}$$

Then Eq. (S6) can be written as:

$$\eta = \frac{\left(2t_+ - 1\right)\frac{V_{oc}}{2}}{\frac{R}{F}\ln\frac{\left(C_H\gamma_H\right)^{T_H}}{\left(C_L\gamma_L\right)^{T_L}}} \quad \text{(S17)}$$

where γ_H and γ_H are the ionic activity coefficients at the high and low concentrations, respectively, and their values are [S3]:

$$\log\left(\gamma_{H(L)}\right) = \frac{-0.511I_s^{1/2}}{1 + I_s^{1/2}} + \frac{\left(0.06 + 0.6B\right)I_s}{\left(1 + 1.5I_s\right)^2} + BI_s \quad \text{(S18)}$$

where I_s is the ionic strength, and for KCl solution, $B = 0.024$.

4. Data supplement

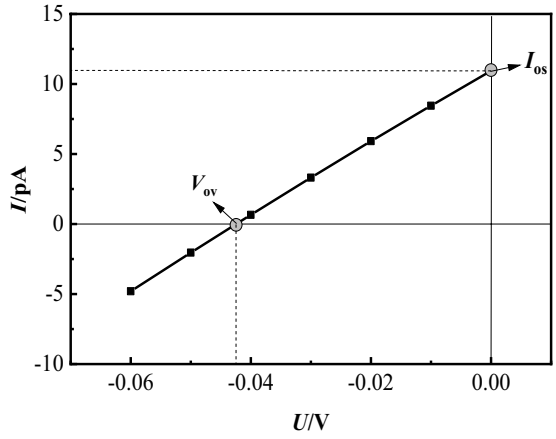

Fig. S3. Relationship of current and applied voltage. KCl solution, R_H = 100 nm, R_L = 5 nm, h = 500 nm, $T_H = T_L$ = 300 K, $C_H|C_L$ = 10|1.

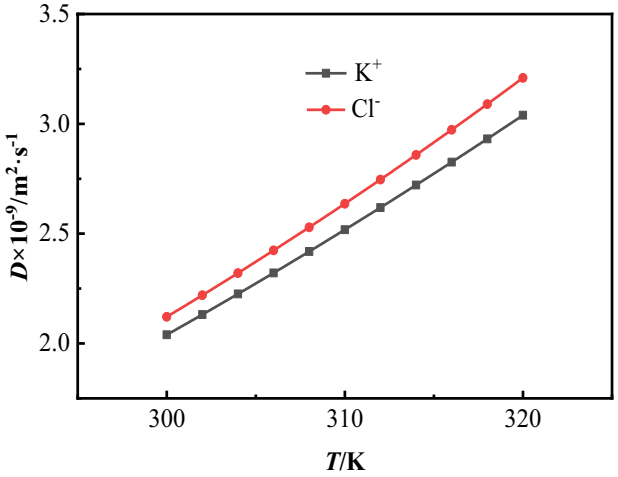

Fig. S5. Variation of diffusivity of K^+ and Cl^- with temperature.

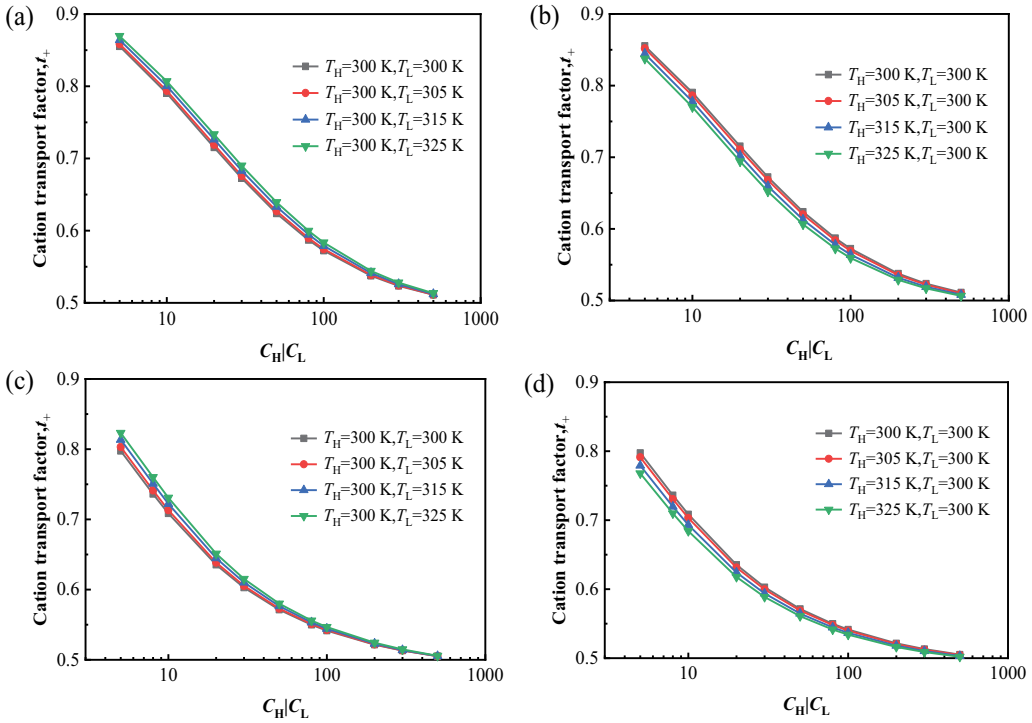

Fig. S4. Variation of cation transport factor of conical nanochannel with the concentration gradients and temperature gradients. (a) NTG, R_H = 100 nm, R_L = 10 nm, h = 500 nm, (b) PTG, R_H = 100 nm, R_L = 10 nm, h = 500 nm, (c) NTG, R_H = 10 nm, R_L = 100 nm, h = 500 nm, and (d) PTG, R_H = 10 nm, R_L = 100 nm, h = 500 nm.

References

[S1] M. Van-Phung, R.-J. Yang, Boosting power generation from salinity gradient on high-density nanoporous membrane using thermal effect, Appl. Energy, 274 (2020) 115294, doi: 10.1016/j.apenergy.2020.115294.

[S2] F. Xiao, D. Ji, H. Li, J. Tang, Y. Feng, L. Ding, L. Cao, N. Li, L. Jiang, W. Guo, Simulation of osmotic energy conversion in nanoporous materials: a concise single-pore model, Inorg. Chem. Front., 5 (2018) 1677–1682.

[S3] J. Cervera, A. Alcaraz, B. Schiedt, R. Neumann, P. Ramirez, Asymmetric selectivity of synthetic conical nanopores probed by reversal potential measurements, J. Phys. Chem. C, 111 (2007) 12265–12273.